View metadata, citation and similar papers at core.ac.uk
brought to you by CORE
provided by National Tsing Hua University Institutional Repository

JOURNAL OF APPLIED PHYSICS 97, 054310 (2005)

Effect of boron doping on the electron-field-emission properties of nanodiamond films

Yen-Chih Lee and Su-Jien Lin
Department of Materials Science and Engineering, National Tsing-Hua University, Hsinchu, Taiwan 300, Republic of China

I-Nan Lin
Department of Physics, Tamkang University, Tamsui, Taiwan 251, Republic of China

Hsiu-Fung Cheng[a]
Department of Physics, National Taiwan Normal University, Taiwan 106, Republic of China

(Received 25 August 2004; accepted 30 November 2004; published online 16 February 2005)

The electron-field-emission (EFE) behavior of the nanodiamond films was observed to be pronouncedly superior to that of the diamond films with micrometer- or submicrometer-sized grains, which is ascribed to the presence of abundant grains boundaries with sp^2 bonds. Incorporation of boron species into the nanodiamond films further improves the EFE properties for the films. The best EFE properties achieved are turn-on field $E_0 = 18\ \mathrm{V}/\mu\mathrm{m}$ with EFE capacity $J = 0.7\ \mathrm{mA}/\mathrm{cm}^2$ at around 30 V/μm applied field. However, boron doping into the nanodiamond films does not result in consistent boron-content dependence of the EFE properties for the films as those in conventional micrometer-sized diamonds. The complication is explained by the fact that the small size of the diamond grains (~20 nm) may not be able to accommodate the boron species into the lattices to effectively act as acceptor dopants. Moreover, the formation of aggregates of the nanosized diamond grains may alter the local field enhancement factor, which further complicates the correlation of the field-emission behavior with the boron-doping concentration for the nanodiamond films. © *2005 American Institute of Physics*. [DOI: 10.1063/1.1852068]

I. INTRODUCTION

Diamond films have attracted considerable scientific attention as electron-field-emission (EFE) materials due to hardness to withstand ion bombardment, and good thermal and electrical conductivity to handle high current.[1–10] Moreover, diamonds in microtip geometry have been shown capable of reducing the turn-on field and achieving large FE current density, which are comparable to those of carbon nanotubes (CNTs).[11–13] Another advantage of diamond films, in terms of FE applications, is that these films can be synthesized easily by using microwave plasma-enhanced chemical vapor deposition (MPECVD) process with consistent EFE properties. In contrast, CNTs, although possessing superior EFE properties to the diamond films, have poor processing reliability, since the preparation of CNTs involves catalysts[14] in the synthesizing process. Therefore, there has been wide interest in improving the EFE properties of diamond films recently. One of the possible routes for increasing the EFE capacity of diamond films is to increase the proportion of grain boundary region, as it has been proposed that the grain boundaries contain sp^2 bond[15] and provide conduction path for electron, facilitating the EFE process. Increasing nucleation density is of critical importance for the purpose of synthesizing nanodiamonds. Various techniques have been applied to enhance the nucleation rate for growing diamond films.[16–18] The bias-enhanced nucleation (BEN) process is overwhelmingly advantageous to these prenucleation processes[19–21] and can achieve a very high nucleation density. Recently, Sharda *et al.*[22] and Jiang *et al.*[23] extended the bias voltage over growing period, which markedly enhanced the secondary nucleation and lead to the formation of nanodiamond films.

In the present work, we adopted the bias-enhanced technique for promoting the nucleation of nanodiamonds and suppressing the growth of grains. The effects of growth parameters in a CVD process on the microstructure and crystal structure of the diamond films were systematically studied. These characteristics were then correlated with the EFE properties of the films and a possible mechanism was discussed.

II. EXPERIMENTAL METHODS

The diamond films were grown in a 2.45 GHz ASTeX MPECVD system on *p*-type mirror-polished Si(100) substrates. No pretreatment on substrate was performed prior to the depositions of diamond films. The substrate assembly was immersed in methane and hydrogen plasma. The nucleation of diamonds was carried out under continuous negative dc bias voltage, from −100 or −175 V, to the substrate. The details of the deposition parameters for each series of samples are listed in Table I. The films were characterized using Raman spectroscope (Renishaw, 514.5 nm) and field-emission scanning electron microscope (Jeol). EFE from diamond films were measured using an electron source unit (Keithley, Model 237).

[a]Author to whom correspondence should be addressed; electronic mail: hfcheng@phy03.phy.ntnu.edu.tw

 © 2005 American Institute of Physics

Downloaded 19 Dec 2010 to 140.114.66.106. Redistribution subject to AIP license or copyright; see http://jap.aip.org/about/rights_and_permissions

TABLE I. The deposition parameters used for nucleation and growth of the diamonds in MPECVD process.[a]

	Total Pressure		Microwave power		CH_4/H_2		Bias	
Materials	N^c (Torr)	G^c (Torr)	N (W)	G (W)	N (%)	G (%)	N (V)	G (V)
Series A (U-dia)[b]	72	72	1700	1700	3	2	−100	0
Series B (S-dia)[b]	75	75	1750	1750	3	2	−100	0
Series C (N-dia)[b]	55	55	1500	1500	5	5	−175	−175

[a]Hydrogen flow rate: 300 sccm.
[b]U-dia: diamonds of micrometer-sized grains; S-dia: diamonds of submicrometer-sized grains; N-dia: diamonds of nanosized grains.
[c]N: CVD parameters in nucleation stage; G: CVD parameters in growth stage.

In a previous report, we observed that, while the bias voltage was held constant during the nucleation period in MPECVD process, the bias current increased abruptly after some incubation period, which had been ascribed to the enhancement in electron emission from the silicon substrate surface as highly emissive diamond is present.[24,25] The time interval before the abrupt increase in bias current is thus designated as the incubation time for the formation of diamond nuclei.

III. RESULTS AND DISCUSSION

The morphology of the diamond films changes pronouncedly with the CVD parameters during the nucleation and growth stages in the MPECVD process. The grains of the diamond films can be either of micrometer size [Fig. 1(a)] or submicrometer size [Fig. 1(b)], when the films were grown under 0 V bias voltage after BEN stage (series A and B, Table I). Extending the bias voltage all the way through the growth stage (series C, Table I) can effectively promote the formation of diamond nuclei on top of the existing diamond grains, resulting a diamond film with nanosized grains, that is, forming the nanodiamond [Fig. 1(c)]. Raman spectra shown in Fig. 2(a) reveals that the diamonds with micrometer grains have a sharp resonance peak at $1332\ cm^{-1}$, whereas those with submicrometer and nanosized grains have a D^* band at $1140\ cm^{-1}$ and G^* band at $1480\ cm^{-1}$, in addition to the broad D band at $1332\ cm^{-1}$. Apparently, the D^*-band and G^*-band Raman resonance peaks are associated with the nanodiamond.

The EFE properties for these diamond films vary significantly with the microstructure. Figure 2(b) reveals that the films of micrometer diamonds are essentially none emitting, whereas the films of submicrometer diamonds can be turned on at around $E_S=42\ V/\mu m$ and achieve EFE current density $J_S=290\ \mu Acm^2$ at around 85 $V/\mu m$ applied field. The nanodiamonds exhibit even better EFE properties. That is, they can be turned on at $E_N=17\ V/\mu m$, achieving $J_N=475\ \mu A/cm^2$ EFE capacity at 35 $V/\mu m$ applied field. It should be noted that all the diamond films are nondoped. The relatively large EFE capability for the nanodiamonds can only be attributed to the presence of large proportion of grain boundaries, which are of sp^2 bonded and are good conductors, facilitating the transport of electrons and acting as EFE sites.[25,26]

To further improve the EFE properties of the films, 0–3 sccm $B(OCH_3)_3$ species were added to the reaction gases so as to incorporate the boron species into the nanodiamonds as acceptor dopants, because previous reports showed that the electrical conductivity of the materials would be markedly increased when a proper amount of boron species were incorporated into the diamond films.[26] Figure 3(a) reveals that addition of $B(OCH_3)_3$ species in the reaction gases moderately alters the bias current-time characteristics (under −175 V bias voltage), that is, the presence of boron species enhances slightly the rate of nucleation for the sp^3 bonds. However, the Raman spectra seem not be modified at all due to the incorporation of B species. All the Raman spectra contain a D^* band ($1140\ cm^{-1}$), representing the presence of nanosized diamond grains, the D band ($1332\ cm^{-1}$) for diamonds and G band ($1580\ cm^{-1}$) for graphitic species [Fig. 3(b)]. Typical scanning electron microscopy (SEM) microstructure for these nanodiamond films is illustrated in Fig. 3(c), which indicates that the films contain diamond grains about 20 nm in size. The microstructure of the nanodiamond films also varies insignificantly with the boron content for the films, except that the average grain size for the films decreases monotonously with the boron content [Fig. 4(a)].

While the Raman spectra and SEM microstructure for the nanodiamond films are insensitive to the amount of boron species incorporated, the EFE properties vary markedly with the boron content for the films. Figure 4(b) shows that all the boron-doped nanodiamond films possess relatively good EFE properties. The turn-on field (E_0) first decreases with boron content, showing the smallest E_0 value for the 1.5 sccm $B(OCH_3)_3$ samples, and increases again when overdoped. The EFE capacity for 0 sccm $B(OCH_3)_3$ containing films achieves $1.0\ mA/cm^2$ for a an applied field around $E_{app}\sim 90\ V/\mu m$). The 1.5 sccm $B(OCH_3)_3$ diamond films exhibit the best EFE properties, which are turn-on field $E_0=18\ V/\mu m$ with EFE capacity $J=0.7\ mA/cm^2$ at around 30 $V/\mu m$ applied field. However, the EFE properties for these nanodiamond films do not vary in a regular manner with respect to the boron content, which is contradictory to the phenomenon observed in the conventional diamond films with micrometer-sized grains; namely, that the field emission properties of the films increases monotonously with boron content.[27] The probable explanation for such a phenomenon is that, in conventional diamond films, the incorporated borons substitute the lattice carbons, acting as acceptor dopants, whereas in nanodiamonds, the grains are too small to accommodate the boron atoms into the lattices, as it induces

Downloaded 19 Dec 2010 to 140.114.66.106. Redistribution subject to AIP license or copyright; see http://jap.aip.org/about/rights_and_permissions

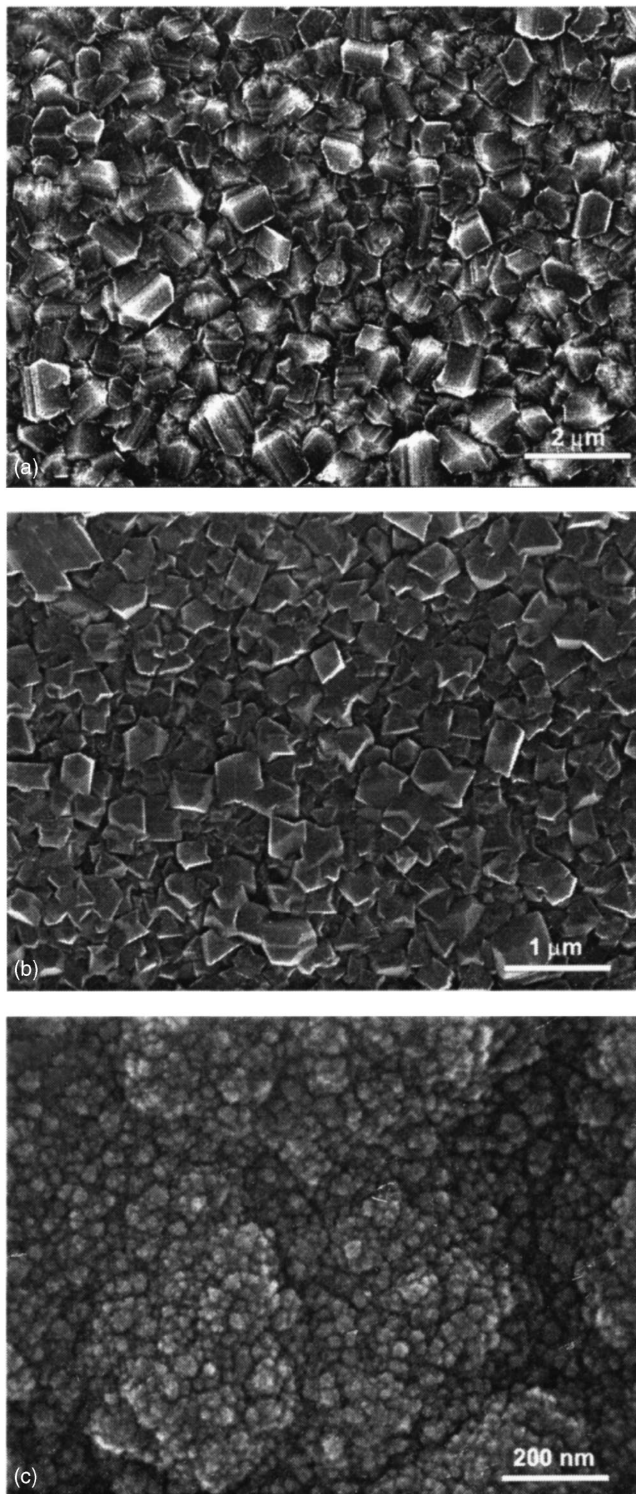

FIG. 1. SEM microstructure for the diamond films with (a) micrometer-sized grains, (b) submicrometer-sized grains and (c) nanosized grains, which are processed using the MPECVD parameters listed in Table I.

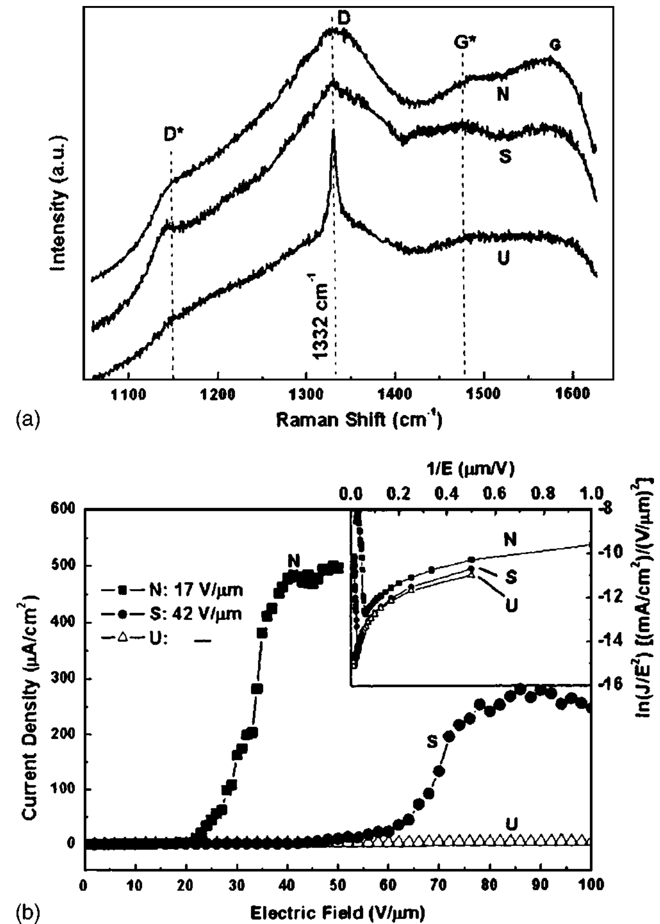

FIG. 2. (a) Raman Spectra and (b) EFE properties for the diamond films with micrometer-sized grains (U), submicrometer-sized grains (S) and nanosized grains (N).

too large a strain. The large proportion of the boron species added are possible sitting at the grain boundaries, so that the EFE properties for the films do not consistently vary with the amount of borons incorporated.

Presumably, the grain boundaries for the nanodiamond films are sp^2 bonded, and are thus highly conducting, facilitating the field emission for the electrons.[25] Nanodiamond films with smaller grain size contain more abundant grain boundaries and are thus expected to possess better EFE properties. However, Figs. 4(a) and 4(b) do not show the direct correlation for the grain size of the films with the EFE properties of the materials. The possible cause resulting in inconsistency for the grain-size dependence of the EFE properties is the complication of the microstructure. As shown in Fig. 3(c), the nanosized diamond grains form uniform aggregates about 200 nm in size. Formation of aggregates results in nonuniformity in the electrical field enhancement factor experienced by individual diamond grains, which complicates the EFE process. Moreover, the diamond grains synthesized under large bias voltage (−175 V) may subject to bombardment damage, as the incident C^+ and H^+ species possess quite large kinetic energy under such a large bias voltage. Formation of amorphous carbons on the surface due to bombardment of energetic C^+ and H^+ species will apparently retard the EFE process. Such an assumption, however, cannot be resolved by the Raman spectroscopy and deserves more detailed investigation in the near future.

IV. CONCLUSION

In summary, variation of the electron-field-emission behavior of the nanodiamond films with the granular structure or the boron doping level was systematically examined. The EFE behavior of the nanodiamond films was observed to be

Downloaded 19 Dec 2010 to 140.114.66.106. Redistribution subject to AIP license or copyright; see http://jap.aip.org/about/rights_and_permissions

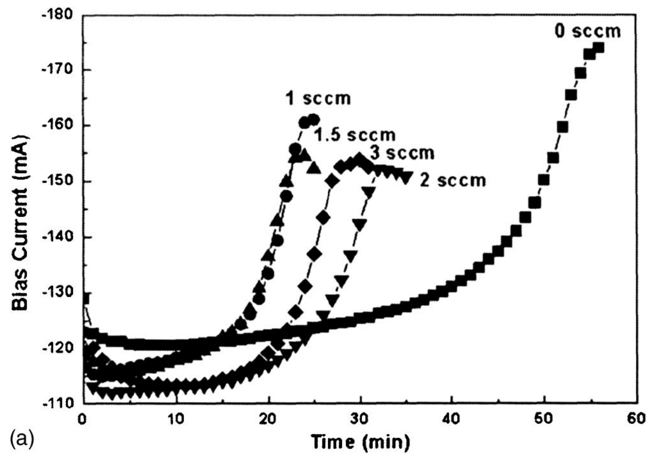

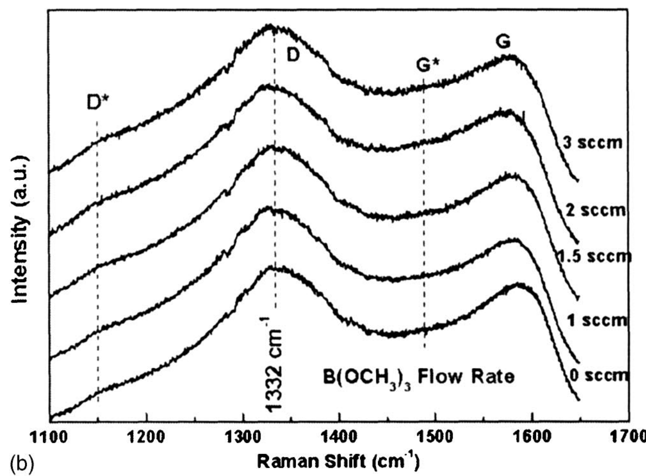

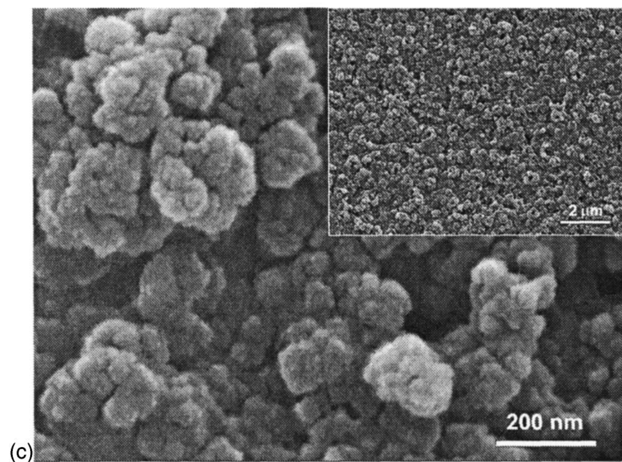

FIG. 3. (a) Bias current-time (I_{bias}-t), (b) Raman spectra, and (c) typical SEM microstructure of the boron-doped nanodiamond films.

pronouncedly superior to that of the diamond films with micrometer- or submicrometer-sized grains, which is ascribed to the presence of abundant grain boundaries with sp^2 bonds. In contrast, boron doping into the nanodiamond films improved their EFE properties remarkably, but did not result in consistent variation on the EFE properties for the films as that in conventional micrometer sized diamonds. The complication was explained by the small size of the diamond grains ($\sim$20 nm) and the formation of aggregates for the nanosized diamond grains.

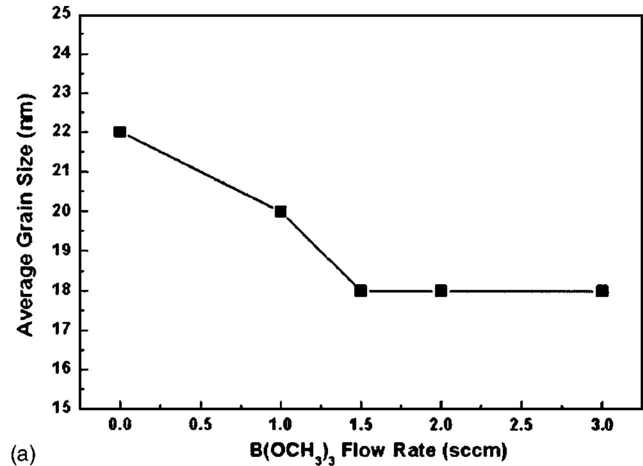

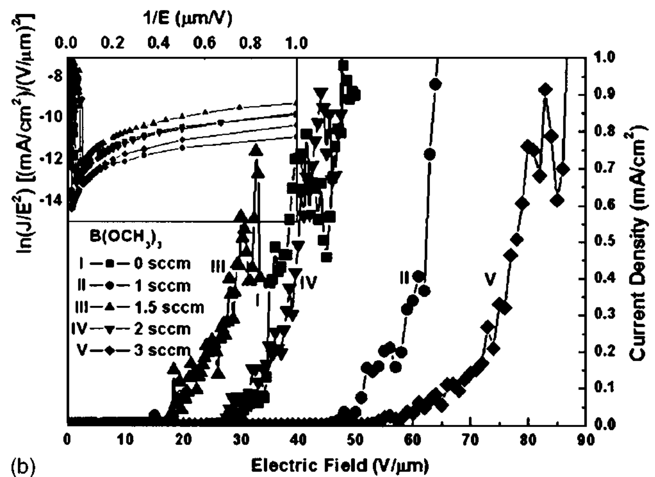

FIG. 4. The variation of (a) grain size and (b) EFE properties of the nanodiamond films with the boron content for the films.

ACKNOWLEDGMENT

The authors would like to thank National Science Council, Republic of China for the support of this research through the project nos. NSC 93-2216-E-003-001 and NSC 92-2216-E-032-005.

[1] C. A. Spindt, I. Brodie, C. E. Holland, and P. R. Schwoebel, in *Vacuum Microelectronics* (Wiley, New York, 2001), p. 105.
[2] F. S. Baker, A. R. Osborn, and J. Williams, Nature (London) **239**, 96 (1972).
[3] M. W. Greis, N. N. Efremow, J. D. Woodhouse, M. N. McAleese, M. Marchywka, D. G. Socker, and J. F. Hochedez, IEEE Electron Device Lett. **12**, 456 (1991).
[4] W. Zhu, P. K. Baumann, C. A. Bower, in *Vacuum Microelectronics* (Wiley, New York, 2001), p. 247.
[5] V. V. Zhirnov, O. M. Küttel, O. Gröening, A. N. Alimova, P. Y. Detkov, P. I. Belobrov, E. Maillard-Schaller, and L. Schlapbach, J. Vac. Sci. Technol. B **17**, 666 (1999).
[6] A. A. Talin, K. A. Dean, and J. E. Jaskie, Solid-State Electron. **45**, 963 (2001).
[7] W. I. Milne, Appl. Surf. Sci. **146**, 262 (1999).
[8] J. Robertson, Mater. Sci. Eng., R. **37**, 129 (2002).
[9] P. K. Bachmann, V. V. Elsbergen, D. U. Wiechert, G. Zhong, and J. Roberson, Diamond Relat. Mater. **10**, 809 (2001).
[10] O. Gröning, L. O. Nilsson, P. Gröning, and L. Schlapbach, Solid-State Electron. **45**, 929 (2001).
[11] W. P. Kang, J. L. Davidson, A. Wisitsora-at, M. Howell, A. Jamaludin, Y. M. Wong, K. L. Soh, and D. V. Kerns, J. Vac. Sci. Technol. B **21**, 593 (2003).

Downloaded 19 Dec 2010 to 140.114.66.106. Redistribution subject to AIP license or copyright; see http://jap.aip.org/about/rights_and_permissions

[12]A. Wisitsora-at, W. P. Kang, J. L. Davidson, D. V. Kerns, and T. Fisher, J. Vac. Sci. Technol. B **21**, 614 (2003).
[13]Y. Ando, Y. Nishibayashi, H. Furuta, K. Kobashi, T. Hirao, and K. Oura, Diamond Relat. Mater. **12**, 1681 (2003).
[14]Y. C. Chen, H. F. Cheng, Y. S. Hsieh, and Y. M. Tsau, J. Appl. Phys. **94**, 7739 (2003).
[15]D. M. Gruen, Annu. Rev. Mater. Sci. **29**, 211 (1999).
[16]S. Iijima, Y. Aikawa, and K. Baba, Appl. Phys. Lett. **57**, 2646 (1990).
[17]J. H. Je and G. Y. Lee, J. Mater. Sci. **27**, 6324 (1993).
[18]S. M. Pimenov, A. A. Smolin, V. G. Ralchenko, V. I. Konov, S. V. Likhanski, and I. A. Veselovski, Diamond Relat. Mater. **2**, 291 (1993).
[19]S. Yugo, T. Kanai, T. Kimura, and T. Muto, Appl. Phys. Lett. **58**, 1036 (1991).
[20]B. R. Stoner, G. H. Ma, S. D. Woltor, and J. T. Glass, Phys. Rev. B **45**, 11067 (1992).
[21]R. Stöckel, M. Stammler, K. Janischowsky, L. Ley, M. Albercht, and H. P. Strunk, J. Appl. Phys. **83**, 531 (1998).
[22]T. Sharda, M. Umeno, T. Soga, and T. Jimbo, Appl. Phys. Lett. **77**, 4304 (2000).
[23]N. Jiang, K. Sugimoto, K. Nishimura, Y. Shintani, and A. Hiraki, J. Cryst. Growth **242**, 362 (2002).
[24]J. S. Lee, K. S. Liu, and I. N. Lin, Appl. Phys. Lett. **67**, 1555 (1995).
[25]I. N. Lin, K. Perng, and L. H. Lee, Appl. Phys. Lett. **77**, 1277 (2000).
[26]Y. H. Chen, C. T. Hu, and I. N. Lin, Appl. Phys. Lett. **75**, 2857 (1999).
[27]Y. H. Chen, C. T. Hu, and I. N. Lin, Appl. Phys. Lett. **75**, 1 (1999).

Downloaded 19 Dec 2010 to 140.114.66.106. Redistribution subject to AIP license or copyright; see http://jap.aip.org/about/rights_and_permissions